Urinary Bladder Cancer: Diffusion-weighted MR Imaging—Accuracy for Diagnosing T Stage and Estimating Histologic Grade[1]

Mitsuru Takeuchi, MD
Shigeru Sasaki, MD, PhD
Masato Ito, MD, PhD
Shinsuke Okada, MD
Satoru Takahashi, MD, PhD
Tatsuya Kawai, MD
Kaori Suzuki, MD
Hidekazu Oshima, MD, PhD
Masaki Hara, MD, PhD
Yuta Shibamoto, MD, PhD

Purpose: To prospectively evaluate the ability of diffusion-weighted (DW) magnetic resonance (MR) imaging to be used to determine the T stage of bladder cancer and to measure the correlation between the apparent diffusion coefficient (ADC) and histologic grade.

Materials and Methods: This study was approved by the local institutional review board. All patients gave written informed consent. Forty patients with a total of 52 bladder tumors underwent MR imaging that included DW imaging. Histologic grade was determined for all tumors. Two radiologists interpreted four image sets (ie, T2-weighted images alone, T2-weighted plus DW images, T2-weighted plus dynamic contrast agent–enhanced images, all three image types together). Conventional criteria were used for interpreting T2-weighted and contrast-enhanced images. For DW images, new staging criterion developed on the basis of the hypothesis that tumors, submucosal tissue, and muscles show high, low, and intermediate signal intensity, respectively, was used. The McNemar test was used to examine differences in accuracy, sensitivity, and specificity. Differences in the performance were analyzed by comparing the areas under the receiver operating characteristic curves (A_z values). To compare ADCs between three histologic grades, analysis of variance was used.

Results: The overall accuracy of T stage diagnosis was 67% for T2-weighted images alone, 88% for T2-weighted plus DW images, 79% for T2-weighted plus contrast-enhanced images, and 92% for all three image types together. The overall accuracy, specificity, and A_z for diagnosing T2 or higher stages were significantly improved by adding DW images ($P < .01$). The mean ADC of G3 tumors was significantly lower than that of G1 and G2 tumors ($P < .01$).

Conclusion: DW images provided useful information for evaluating the T stage of bladder cancer, particularly in differentiating T1 or lower tumors from T2 or higher tumors. The ADC may in part predict the histologic grade of bladder cancer.

[1] From the Departments of Radiology (M.T., S.S., M.I., T.K., K.S., M.H., Y.S.), Nephro-Urology (S.O.), and Experimental Pathology and Tumor Biology (S.T.), Nagoya City University Graduate School of Medical Sciences, 1 Kawasumi Mizuho-cho, Mizuho-ku, Nagoya 467-8601, Japan; and Department of Radiology, Inabe General Hospital, Inabe, Japan (H.O.). From the 2007 RSNA Annual Meeting. Received May 19, 2008; revision requested July 2; revision received October 1; accepted October 24; final version accepted November 4. Supported in part by Grants-in-Aid for Scientific Research from the Japanese Ministry of Education, Culture, Sports, Science, and Technology. **Address correspondence to** M.T. (e-mail: *m2rbimn@gmail.com*).

Clinical management of urinary bladder cancer is determined primarily on the basis of distinguishing superficial tumors (stage T1 or lower) from invasive ones (stage T2 or higher) because the treatment options differ considerably. Superficial tumors are treated with transurethral resection (TUR) with or without adjuvant intravesical chemotherapy or photodynamic therapy (1), whereas invasive tumors are treated with radical cystectomy, radiation therapy, chemotherapy, or a combination (2). Therefore, preoperative imaging studies would play an important diagnostic role if they could be used to precisely differentiate between the two categories of bladder cancer. Dynamic magnetic resonance (MR) imaging appears to be more useful than computed tomography for staging bladder cancer (3–9), but overstaging has been reported to be a common error when using dynamic MR imaging (3). Contrast agents can have adverse effects, including nephrogenic systemic fibrosis (10). Transurethral endoscopic ultrasonography is more invasive. Therefore, further improvement of a diagnostic modality may be desirable.

Advances in Knowledge

- Submucosal components showed low signal intensity on diffusion-weighted (DW) MR images, representing a mixture of markedly edematous submucosa, fibrous tissue, capillaries, and mild inflammatory cell infiltration.
- The accuracy for diagnosing the T stage of bladder cancer was significantly improved when DW images were viewed together with T2-weighted images ($P = .006$).
- The specificity for differentiating T1 or lower tumors from T2 or higher tumors was significantly improved when DW images were viewed with T2-weighted images ($P = .004$).
- The apparent diffusion coefficients (ADCs) of G3 tumors were significantly lower than those of G1 and G2 tumors ($P < .01$).

The usefulness of diffusion-weighted (DW) MR imaging for depicting malignant tumors (11–16) and an apparent diffusion coefficient (ADC) (17–23) for characterizing tumor grades have been suggested recently. Matsuki et al (24) reported that the ADCs of urinary bladder cancers were lower than those of surrounding structures and that the tumors were clearly depicted as lesions with high signal intensity (SI) on DW images. We conducted this study to prospectively evaluate the usefulness of DW imaging for determining T stage for bladder cancers and to measure the correlation between ADC and histologic grade.

Materials and Methods

Study Design

Approval for the study was obtained from the local institutional review board. Written informed consent was obtained from all patients. The diagnostic accuracy of dynamic MR images for staging bladder cancer has been reported to be between 52% and 93% (3–9). If the accuracy of dynamic MR imaging is assumed to be 75%, a total of 40 tumors was considered to be required to detect differences of 20% between dynamic MR imaging alone and dynamic plus DW MR imaging with a significance level of .05 and a statistical power of 80%.

Patient Population

Between July 2006 and November 2007, 64 consecutive patients who were suspected of having bladder cancer and who did not have impaired renal function underwent contrast agent–enhanced MR imaging. All 64 patients underwent TUR or transurethral biopsy after imaging, and seven patients were excluded because bladder cancer was not proved. Seventeen other patients were excluded because their cancers appeared to be clinically noninvasive, but it was not histologically confirmed whether the tumors were invasive or noninvasive. The remaining 40 patients formed the basis of this report. Noninvasive bladder cancer was proved in 23 patients, and invasive bladder cancer was proved in 17. Four of the 23 patients with noninvasive cancer and 13 of the 17 patients with invasive cancer underwent radical cystectomy (Fig 1). Patients with tumors invading the muscle or intravesical chemotherapy–resistant multiple relapses, good cardiopulmonary function, and good performance status and without nodal and distant metastases were considered to be candidates for radical cystectomy.

Pathologic stage was determined in 40 patients (age range, 49–85 years; mean, 70 years). There were 34 men (age range, 49–83 years; mean, 70 years) and six women (age range, 63–85 years; mean, 73 years). Eight pa-

Implications for Patient Care

- DW imaging may be useful in treatment planning and in determining the prognosis in patients with bladder cancer.
- The excellent specificity of DW images (97%) for enabling diagnosis of muscle invasion would help guide therapeutic planning.
- The presence of a low ($<1 \times 10^{-3}$ mm^2/sec) ADC could indicate that the tumor is more likely to be G3.

Published online
10.1148/radiol.2511080873

Radiology 2009; 251:112–121

Abbreviations:
ADC = apparent diffusion coefficient
A_z = area under the receiver operating characteristic curve
DW = diffusion weighted
SI = signal intensity
SLE = submucosal linear enhancement
TUR = transurethral resection

Author contributions:
Guarantors of integrity of entire study, M.T., M.I., M.H., Y.S.; study concepts/study design or data acquisition or data analysis/interpretation, all authors; manuscript drafting or manuscript revision for important intellectual content, all authors; approval of final version of submitted manuscript, all authors; literature research, M.T.; clinical studies, M.T., S.S., M.I., S.O., S.T., T.K., K.S., M.H.; statistical analysis, M.T., H.O.; and manuscript editing, M.T., M.H., Y.S.

Authors stated no financial relationship to disclose.

tients had multiple tumors (12 additional tumors), so a total of 52 tumors were analyzed. All patients underwent surgery within 41 days (mean, 7 days) after MR imaging. In patients who underwent TUR, an additional deep muscle biopsy was performed at the base of the tumor. When no tumor cells were found, the pathologic stage was classified as T1 or less. Twelve to 140 days (median, 98 days) before the MR examination, 16 (40%) of 40 patients had undergone transurethral biopsy intravesical chemotherapy, systemic chemotherapy, or a combination of these two methods.

MR Imaging Technique

To moderately distend the bladder, all patients were prohibited from urinating for at least 1 hour before examination. To reduce bowel motion, 18 (45%) of the 40 patients received 20 mg of scopolamine butylbromide (Buscopan; Boehringer Ingelheim, Tokyo, Japan), and five (12%) received 1 mg of glucagon (Glucagon G Novo; Novo Nordisk Pharma, Tokyo, Japan). The remaining 17 (42%) patients had a contraindication to the drug regime or rejected antispasmodic agents.

MR imaging was performed by using a 1.5-T imager (Gyroscan Intera; Philips Medical Systems, Best, the Netherlands) with a maximum amplitude of the gradients of 33 mT/m and a maximum slew rate of 180 T/m/sec and equipped with a radiofrequency coil (Quadrature body coil; Philips Medical Systems) and a phased-array 5-channel sensitivity encoding cardiac coil (Philips Medical Systems).

Turbo spin-echo T2-weighted images (repetition time msec/echo time msec, 4390–5424/120; matrix, 256 × 189; section thickness, 4 mm; gap, 0.4 mm; number of sections, 19–24; acquisition time, 91–117 seconds; field of view, 23 cm; sensitivity encoding factor, 1.5) and DW images were obtained in the axial and sagittal planes. We also evaluated DW images at a plane perpendicular to the base of tumors, but we found that better signal-to-noise ratios were obtained at axial and sagittal planes than at the perpendicular plane, so axial and sagittal images were used for evaluation. T2-weighted images were also evaluated in the axial and sagittal planes, in accordance with the DW images. The DW images were obtained by using a single-shot spin-echo echo-planar sequence with chemical shift–selective fat-suppression techniques (*b*, 0 and 1000 sec/mm^2 [DW gradients applied in three orthogonal directions]; 2790–4560/88; matrix, 128 × 109; section thickness, 4 mm; gap, 0.4 mm; field of view, 25–33 cm; number of sections, 19–24; number of signals acquired, 14; sensitivity encoding factor, 2; acquisition time, 146–196 seconds). Preliminarily, various numbers of signal acquisitions were evaluated, and this number appeared to be appropriate to yield DW images of sufficient quality. To gain better signal-to-noise ratios, a larger field of view was used for DW imaging than for T2-weighted imaging, and a thicker section was used for T2-weighted and DW imaging than for T1-weighted fast field echo imaging.

T1-weighted fast field-echo images with a water-selective excitation technique (9.8–10.4/4.9–5.2; flip angle, 20°; matrix, 224 × 214; section thickness, 3 mm; gapless; field of view, 35 cm; number of sections, 24–27; sensitivity encoding factor, 2; acquisition time, 26–30 seconds) were obtained before and after administration of 0.2 mL per kilogram of body weight gadopentetate dimeglumine (Magnevist; Bayer Yakuhin, Osaka, Japan) or gadodiamide (Omniscan; Daiichi Sankyo Pharmaceuticals, Tokyo, Japan). It was assumed that the two agents had the same effectiveness for contrast enhancement (25). Dynamic contrast-enhanced images were obtained at planes perpendicular to the base of the tumors. Images were acquired at 30, 60, 90, and 120 seconds after injection of the contrast agent. For all imaging, repetition and echo times were set to be as short as possible, depending on the number of sections and the angle between the body axis and imaging plane; therefore, they were variable.

Figure 1

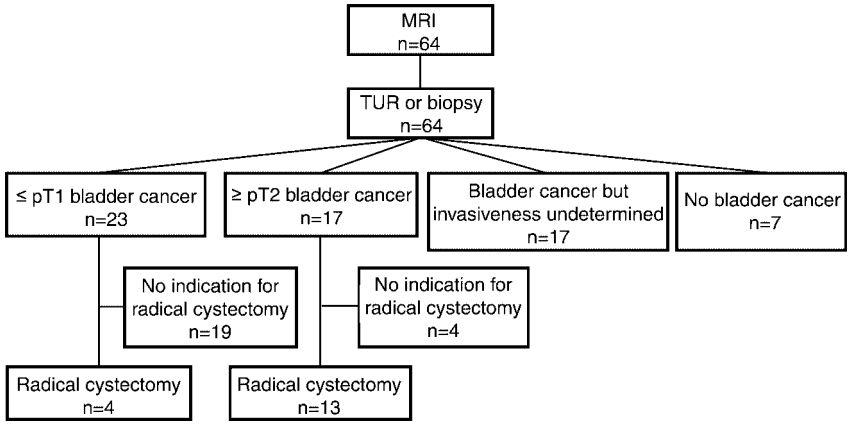

Figure 1: Flow diagram of patients.

Table 1

T Staging for Bladder Cancer

Stage	Description
Tis	Carcinoma in situ
Ta	Papillary noninvasive tumor
T1	Tumor invades subepithelial connective tissue
T2a	Tumor invades superficial muscle
T2b	Tumor invades deep muscle
T3a	Tumor invades perivesical tissue microscopically
T3b	Tumor invades perivesical tissue macroscopically
T4a	Tumor invades prostate, uterus, or vagina
T4b	Tumor invades pelvic or abdominal wall

Source.—Reference 26.

Figure 2

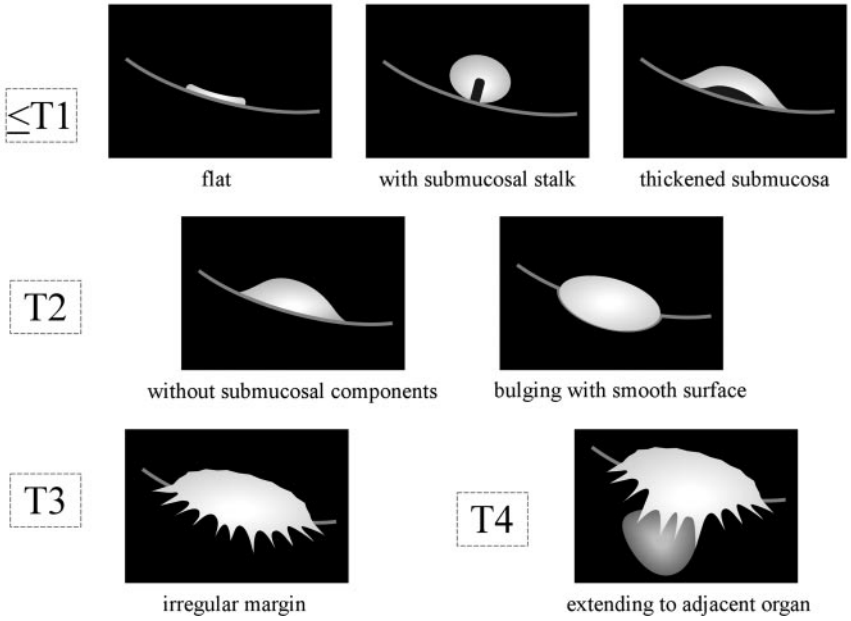

Figure 2: Schematic shows diagnostic criteria for using DW imaging for staging bladder cancer. Cancer component, muscle layer, and submucosa show high, intermediate, and low SI, respectively. Submucosal stalk or thickened submucosa indicates T1 or lower stage; smooth tumor margin without submucosal components, T2; irregular margin toward the perivesical fat tissue, T3; and extension into adjacent organs, T4.

Table 2

Diagnostic Accuracy for Differentiating Stage Tis to T1 Tumors from T2 to T4 Tumors

Image Set	Sensitivity	Specificity	Accuracy
T2 weighted	15/17 (88)	26/35 (74)	41/52 (79)
T2 weighted plus DW	15/17 (88)*	35/35 (100)†	50/52 (96)†
T2 weighted plus contrast enhanced	16/17 (94)	30/35 (86)	46/52 (88)
All three types	16/17 (94)	35/35 (100)†	51/52 (98)†

Note.—Data in parentheses are percentages.

* Note that sensitivity did not improve when DW images were viewed with T2-weighted images.

† $P < .01$ compared with T2-weighted images alone.

Table 3

Diagnostic Accuracy for Differentiating Stage Tis to T2 Tumors from T3 to T4 Tumors

Image Set	Sensitivity	Specificity	Accuracy
T2 weighted	5/10 (50)	36/38 (95)	41/48 (85)
T2 weighted plus DW	7/10 (70)	37/38 (97)	44/48 (92)
T2 weighted plus contrast enhanced	8/10 (80)	35/38 (92)	43/48 (90)
All three types	8/10 (80)	37/38 (97)	45/48 (94)

Note.—Data in parentheses are percentages. There were no significant differences in sensitivity, specificity, or accuracy among the four image sets.

Image Interpretation

All MR image sets were independently reviewed in a random order by two radiologists (M.I. and S.S., with 21 and 15 years experience, respectively). The observers were notified of tumor locations but were blinded to all other information. They reviewed four image sets: T2-weighted images alone, T2-weighted plus DW images, T2-weighted plus contrast-enhanced images, and all three image types together. First, the T2-weighted alone and T2-weighted plus DW image sets were interpreted (in that order), and then the remaining sets (T2-weighted plus contrast-enhanced and all three types together) were evaluated after an interval of 3 weeks. When interpreting all the three image types together, T2-weighted and contrast-enhanced images were mainly used to recognize anatomy, and DW images were used to evaluate the extent of the tumor. Differences in assessment were resolved by means of consensus.

Tumor Staging

The observers were requested to classify the tumors into the following four categories in accordance with the 1997 TNM system of the International Union Against Cancer (26): T1 or lower, T2 (T2a or T2b), T3 (T3a or T3b), and T4 (T4a or T4b) (Table 1). The staging criteria used were similar to those described previously for T2-weighted images (27–29) and contrast-enhanced images (4), and we defined a new criterion for DW images in this study.

Since the normal bladder wall can be seen as a low SI line on T2-weighted images, the bladder wall was considered to be intact (stage T1 or lower) when the low SI line was present. The bladder was considered to be invaded by the tumor (stage T2 or higher) when the low SI line was disrupted focally in the region underlying the tumor (27–30). On contrast-enhanced images, submucosal linear enhancement (SLE) is depicted immediately after the injection of contrast agent, and the SI of the muscle layer remains low. Therefore, an intact SLE adjacent to a tumor was regarded as indicative of stage T1 or lower. When the SLE was disrupted by

a tumor but there was no infiltration into the perivesical fat, this was considered to be stage T2 (4). On both T2-weighted and contrast-enhanced images, tumors invading the perivesical fat were classified as T3, and those extending into an adjacent organ or the abdominal wall, as T4.

On DW images, bladder cancer has been reported to show high SI (24). We assumed that a line of intermediate SI outlining the bladder lumen and a low SI area between the tumor and muscle could reflect a muscle layer and a submucosal stalk, respectively. We proposed a new staging criterion for DW imaging as follows (Fig 2): A thin, flat, high SI area corresponding to the tumor or a high SI tumor with a low SI submucosal stalk or a thickened submucosa indicates stage T1 or lower; a high SI tumor without a submucosal stalk and with a smooth tumor margin indicates stage T2; extension into the perivesical fat with an irregular margin indicates stage T3; and extension into adjacent organs indicates stage T4.

ADC and Histologic Grade

ADC maps were generated at each section in the 41 tumors that were large enough (>5 mm) to contain the region of interest. ADC were measured to estimate the degree of diffusion (31).

Histopathologic Analysis

The specimens were stained with hematoxylin-eosin stain for conventional histopathologic evaluation. All bladder tumors were staged by a pathologist (S.T., with 21 years experience) in accordance with the 1997 International Union Against Cancer system and were defined by using the 1973 World Health Organization classification.

Histologic grading was evaluated with respect to increased cellularity, nuclear crowding, disturbance of cellular polarity, failure of differentiation from the base to the surface, polymorphism, irregularity in the size of cells, variations of shape, chromatin patterns of nuclei, displaced or abnormal mitotic figures, and giant cells. Tumors were classified into three grades: G1, the least degree of anaplasia; G2, an intermediate degree of anaplasia; and G3, severe anaplasia (32).

A radiologist (M.T., with 6 years experience) and the above-mentioned pathologist (S.T.) discussed the correlation between the DW imaging and histopathologic findings.

Statistical Analysis

Interobserver agreement was calculated by using κ statistics. κ Scores of 0.41–0.60, 0.61–0.80, and greater than 0.80 were regarded to be indicative of moderate, good, and excellent agreement, respectively (33).

Diagnostic accuracy of staging with MR images as compared with pathologic stage was assessed on a stage-by-stage basis. Differences in diagnostic accuracy for each image set were evaluated by using the McNemar test with statistical software (SPSS 11.0 for Windows; SPSS Japan, Tokyo, Japan) (34). To compare the utility of each image set for diagnosing muscle invasion (T2 or higher) and perivesical invasion (T3 or higher), receiver operating characteristic curve analyses were performed, and confidence level scores (1 = absent, 2 = probably absent, 3 = possibly present, 4 = probably present, and 5 = present) were assigned. Differences in performance of the four image sets were analyzed by comparing the corresponding area under the receiver operating characteristic curves (A_z) for the mean

Table 4

Overall Accuracy and Interobserver Agreement

Image Set	Accuracy*	κ Value†	*P* Value
T2 weighted	32/48 (67)	0.70 (0.53–0.87)	<.01
T2 weighted plus DW	42/48 (88)‡	0.88 (0.75–1.00)	<.01
T2 weighted plus contrast enhanced	38/48 (79)§	0.55 (0.36–0.72)	<.01
All three types	44/48 (92)‖	0.87 (0.74–1.00)	<.01

* Data in parentheses are percentages.

† Data in parentheses are 95% confidence intervals.

‡ $P = .006$ compared with T2-weighted images alone.

§ $P = .021$ compared with T2-weighted images alone.

‖ $P < .001$ compared with T2-weighted images alone.

Figure 3

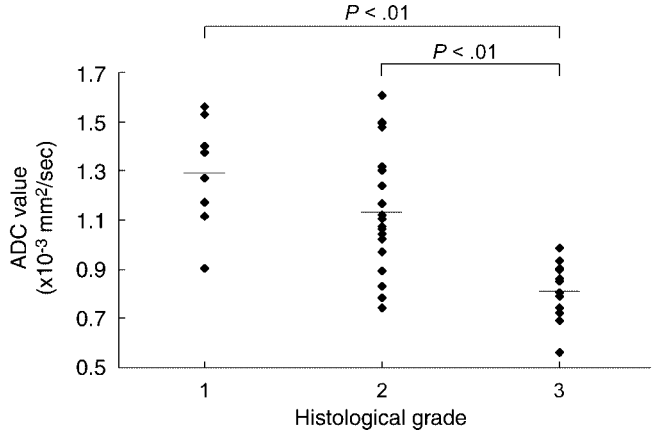

Figure 3: Dot plot of ADC versus histologic grades of urothelial carcinomas. Horizontal tick marks indicate mean ADC for each grade. Significant differences in mean ADC were observed between G1 and G3 ($P < .01$) and between G2 and G3 ($P < .01$) but not between G1 and G2.

score of the two observers (35). These analyses were performed by using software (DBM-MRMC; C. E. Metz, University of Chicago, Chicago, Ill).

To compare the mean ADCs and histologic grade, analysis of variance was used. The post hoc hypothesis testing was performed according to the Fisher protected least significant difference method by using software (StatView, version 5; SAS Institute, Cary, NC).

Results

Tumor Characteristics

Of the 52 tumors, tumor stage was histologically confirmed in 48. In the remaining four tumors resected with TUR, the deep muscle biopsy revealed the invasion of tumor cells. These four tumors were classified as "T2 or higher," and they were not used for evaluating the ability to differentiate T2 and lower tumors from T3 and higher tumors. The pathologic stage was between Tis and T1 in 67% (35 of 52) of tumors, T2 in 6% (three of 52), T3 in 13% (seven of 52), T4 in 6% (three of 52), and "T2 or higher" in 8% (four of 52). The tumors measured 0.4–85.2 mm in maximum diameter (mean, 20.0 mm). Histologic diagnoses were urothelial carcinoma (n = 50), urothelial carcinoma with adenocarcinoma (n = 1), and undifferentiated carcinoma (n = 1). In the undifferentiated carcinoma, the histologic grade was unclassifiable. Excluding that tumor, the histologic grade was G1 in nine (18%) of the 51 tumors, G2 in 28 (55%), and G3 in 14 (27%).

Figure 4

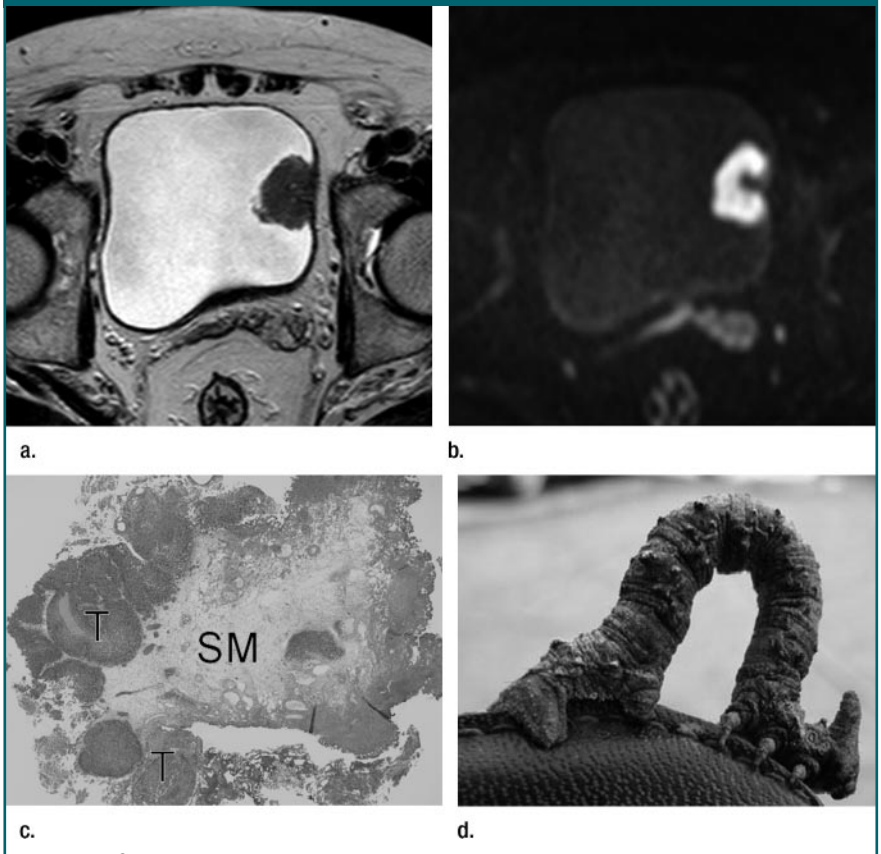

Figure 4: Stage pT1 papillary urothelial carcinoma in a 70-year-old man. **(a)** Transverse T2-weighted MR image shows oval mass on left bladder wall. **(b)** Transverse DW MR image shows C-shaped high SI area with a low SI stalk connecting to left side of bladder wall. **(c)** Photomicrograph of specimen obtained at TUR shows papillary cancer *(T)* with a submucosal stalk *(SM)* consisting of markedly edematous submucosa, fibrous tissue, capillaries, and mild inflammatory cell infiltration. (Hematoxylin-eosin stain; original magnification, ×2.) **(d)** An inchworm creeping along a branch. DW MR imaging finding resembled the archlike shape of an inchworm.

Tumor Staging with MR Images

Sensitivity, specificity, and overall accuracy of the consensus of the two observers for differentiating Tis to T1 tumors from T2 to T4 tumors are summarized in Table 2. Specificities obtained by using T2-weighted plus DW images or all three image types together were significantly better than that obtained by using T2-weighted images alone (P = .004). Accuracies achieved by using T2-weighted plus DW images or all three image types together were also better than that achieved by using T2-weighted images alone (P = .004 and .002, respectively). However, sensitivity was not improved even when DW images were used. The A_z values of T2-weighted images, T2-weighted plus DW images, T2-weighted plus contrast-enhanced images, and all three image types together were 0.87, 0.98, 0.95, and 1.00, respectively. The A_z values of T2-weighted plus DW images, T2-weighted plus contast-enhanced images, and all three image types together were higher than that of T2-weighted images alone (P = .02, .04, and .01, respectively).

Sensitivity, specificity, and accuracy of the consensus of both observers for differentiating T2 or lower tumors from T3 or higher tumors are summarized in Table 3. There were no significant differences among the four image sets. The A_zs of T2-weighted images, T2-weighted plus DW images, T2-weighted plus contrast-enhanced images, and all three image types together were 0.78, 0.93, 0.87, and 0.95, respectively. A significant difference in A_z was only seen between the set of all three image types together and T2-weighted images alone (P = .03).

Interobserver agreement of each interpretation and the overall staging accuracy are summarized in Table 4. Interobserver agreement was excellent for both image sets that included DW images, good for T2-weighted images

Figure 5

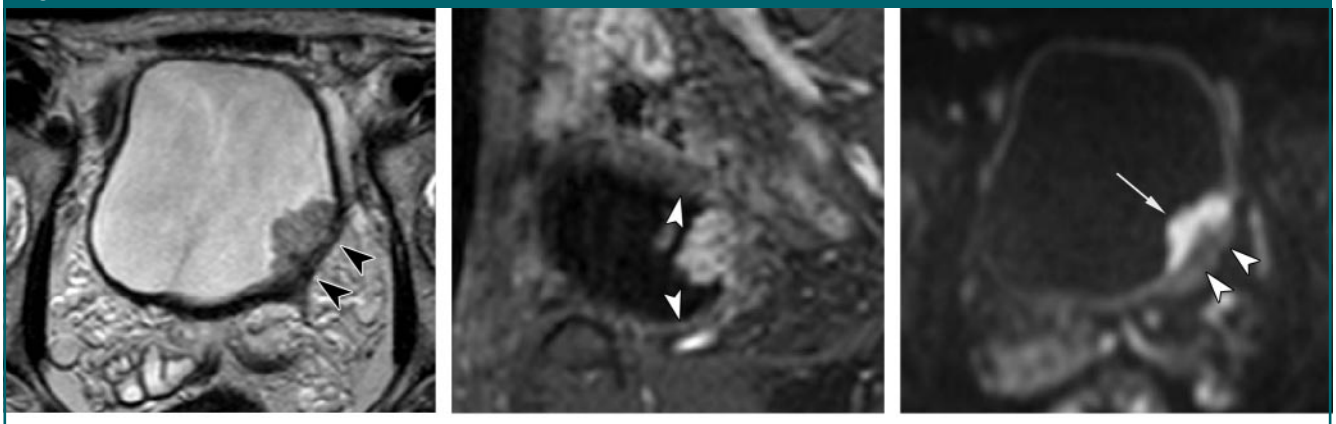

Figure 5: Transverse MR images of a 49-year-old man with pT1 nonpapillary urothelial carcinoma. **(a)** T2-weighted image shows tumor with intermediate SI on left-posterior side of the bladder. SI of muscle layer at base of the tumor is slightly elevated (arrowheads). **(b)** Dynamic contrast-enhanced image shows similarly enhanced indistinguishable structures consisting of tumors and submucosa (arrowheads). **(c)** DW image depicts tumor (arrow) and submucosa (arrowheads) separately, without extension into surrounding muscle.

alone, and moderate for T2-weighted plus contrast-enhanced images. The overall accuracies for diagnosing tumor stage with T2-weighted plus DW images (42 of 48 [88%], $P = .006$), T2-weighted plus contrast-enhanced images (38 of 48 [79%], $P = .021$), and all the three image types together (44 of 48 [92%], $P < .001$) were significantly better than that obtained by using T2-weighted images alone (32 of 48 [67%]).

ADC and Histologic Grade

The correlation between ADC and histologic grade is summarized in Figure 3. The mean ADC of the 41 bladder tumors was (1.07 ± 0.27 [standard deviation]) $\times 10^{-3}$ mm^2/sec. The mean ADCs of G1, G2, and G3 tumors were (1.29 ± 0.21) $\times 10^{-3}$ mm^2/sec (range, [0.91–1.56] $\times 10^{-3}$ mm^2/sec), (1.13 ± 0.24) $\times 10^{-3}$ mm^2/sec (range, [0.74–1.61] $\times 10^{-3}$ mm^2/sec), and (0.81 ± 0.11) $\times 10^{-3}$ mm^2/sec (range, [0.56–0.99] $\times 10^{-3}$ mm^2/sec), respectively. The differences in ADC were significant between G1 and G3 ($P < .01$) and between G2 and G3 ($P < .01$) but not between G1 and G2.

Histopathologic Analysis

Forty-one tumors obtained by using radical cystectomy ($n = 19$) or TUR ($n = 22$) were available for histopathologic correlation. The remaining 11 tumors were not available because these tumors were resected piece by piece at TUR. Histopathologically, the high, intermediate, and low SI areas on DW images corresponded well to tumor, smooth muscle, and edematous submucosa, respectively (Fig 4a–4c). The DW imaging finding of high SI bladder cancer together with a low SI submucosal stalk resembled an archlike inchworm shape and was found in all 28 (100%) patients with pT1 disease (Fig 4b, 4d). In 11 (61%) of the 18 tumors that were diagnosed as pT1 or lower and were larger than 5 mm, the cancer component enhanced as strongly as the submucosal tissue at all dynamic phases, and the area of SLE could not be differentiated from the tumor (Fig 5). Three pT2 tumors showed a smooth or slightly irregular contour and this correlated with pathologic findings (Fig 6a–6c). On DW images, 86% (six of seven) of pT3 tumors showed irregular margins toward the perivesical fat (Fig 7), and the remaining large tumor was accompanied by a small nodule protruding into the perivesical fat.

Discussion

For differentiating between T1 or lower tumors and T2 or higher tumors, the accuracy of dynamic contrast-enhanced MR images has been reported to be 75%–92% (3,4,8), and the overall accuracy for diagnosing tumor stage has been reported to be 52%–93% (3,5–9). In a study by Hayashi et al (4) that which employed an endorectal coil, the diagnostic accuracy of using the criterion of SLE, which we also used, was 87% when differentiating between T1 or lower tumors and T2 or higher tumors, and the overall accuracy for staging bladder tumors was 83%. In our study, the overall staging accuracy was 92% when T2-weighted, contrast-enhanced, and DW images were used together. The accuracy was 98% (51 of 52), which was equal to or slightly better than that in previous reports, suggesting the incremental usefulness of DW imaging. Moreover, the accuracy and specificity we observed when using DW imaging in combination with other techniques appear to be higher than those reported previously. We believe that this was due to the enhanced visibility of the structures of the tumor, muscle layer, and thickened submucosa, all of which showed different SI on DW images. Tsushima et al (11) suggested that the detectability of malignant abdominal tumors would be improved by using DW images when reference could also be made to other

images. In our study, however, DW imaging did not improve the sensitivity for diagnosing pT2 or higher stages. Our results can be explained because the muscle layer was usually depicted as a thin structure on DW images; therefore, the extent of tumor growth into the muscle layer could not be precisely evaluated. In addition, the contrast difference between tumor and muscle layers was not great on DW images, and, as a result, it may be difficult to distinguish invasive from superficial tumors.

Saito et al (36) reported that the stalk extending from the bladder wall to the center of the tumor consisted of fibrous tissues, capillaries, inflammatory cells, and edema. Our histologic evaluation showed that the low SI stalk that appeared on DW images between the tumor and muscle layer corresponded to a mixture of markedly edematous submucosa, fibrous tissue, capillaries, and mild inflammatory cell infiltration. There have been no reports describing how this stalk is formed, but it is thought that the reactive inflammation and edema lift the tumor up and form the stalk as a result. The characteristic finding on DW images of the high SI bladder cancer over the low SI submucosal stalk was an arch-shaped appearance similar to an inchworm. We regarded this characteristic finding to be indicative of a pT1 or lower tumor, so dynamic contrast-enhanced images could be skipped.

Tekes et al (3) reported that 81% of bladder tumors showed an SI similar to that of muscle on T2-weighted images and that overstaging was the most common error when evaluating T stage. We also believed that the insufficient SI contrast between tumor and submucosa might cause relatively low accuracy and low levels of interobserver agreement. In our study, the tumor and submucosa were of similar SI in 60% (31 of 52) of the dynamic contrast-enhanced findings, and SLE was difficult to recognize in these cases. Therefore, contrast-enhanced images might have limitations for use to correctly distinguish pT1 tumors with intact SLE from pT2 tumors with disrupted SLE. DW imaging could reduce overstaging because of its good contrast resolution.

Tekes et al (3) reported a sensitivity and specificity of 86% and 84%, respectively, for discriminating between pT2

Figure 6

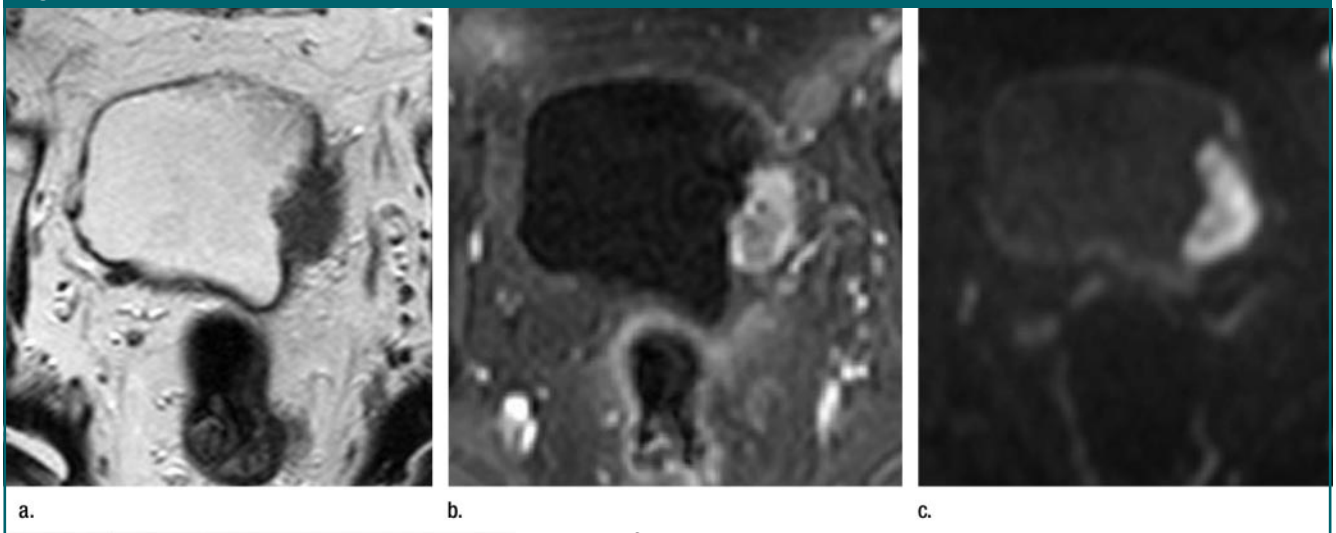

Figure 6: Stage pT2b urothelial carcinoma in a 71-year-old man. **(a)** Transverse T2-weighted MR image shows tumor extending into perivesical fat with an irregular contour. **(b)** Transverse dynamic contrast-enhanced MR image shows tumor bulging into perivesical fat with a slightly irregular contour. **(c)** Transverse DW MR image shows bulging tumor with a smooth margin on left wall of the bladder. **(d)** Photomicrograph of specimen obtained at cystectomy shows nonpapillary bladder cancer *(T)* bulging into perivesical fat *(F)* without disrupting the muscle layer (*M*, arrowheads). (Hematoxylin-eosin stain; original magnification, ×2.)

Figure 7

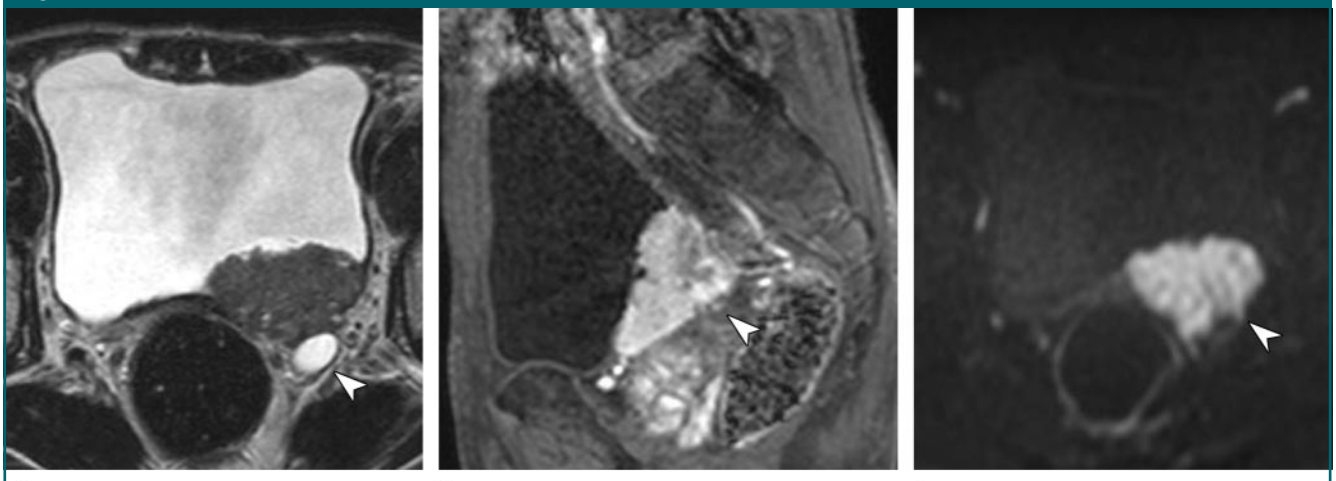

a. b. c.

Figure 7: MR images of a 72-year-old man with pT3b urothelial carcinoma. **(a)** Transverse T2-weighted image shows large nonpapillary tumor on deformed muscle layer with hydroureter (arrowhead). SI of muscle layer at base of the tumor is elevated, but there is no evidence of perivesical invasion. **(b)** Dynamic contrast-enhanced image of oblique section perpendicular to base of tumor does not depict tumor contour because microvessels surrounding the tumor are also enhanced (arrowhead). **(c)** Transverse DW image shows large tumor with irregular margin spreading toward surrounding fat tissue (arrowhead).

or lower tumors and pT3 or higher lesions. Narumi et al (8) reported an overall accuracy of 92%. In our study, the diagnostic accuracy achieved by using all three techniques together for diagnosing pT3 or more advanced tumors was 94% (45 of 48), which is similar to that of previous reports. Tekes et al (3) speculated that the improvement in image resolution might lead to an improvement in the detection of perivesical stranding, which frequently represents reactive or inflammatory changes, rather than a metastatic lesion, but has been occasionally described in the literature as representative of the perivesical spread of tumors. It was also thought that tumor contours could be evaluated more accurately by using DW images because the microvessels or reactive tissue adjacent to the tumor could be enhanced to a level similar to that of a cancer component on contrast-enhanced images but could be distinguished from tumors with the contrast of DW images. In our study, however, the accuracy for differentiating pT2 or lower tumors from pT3 and higher tumors was not improved, even when DW images were evaluated together with T2-weighted images. Nevertheless, DW images could depict smooth or slightly irregular contours in all three pT2 tumors and irregular contours in six of the seven pT3 tumors.

ADCs representing the degree of water molecular diffusion and the degree of restriction to water diffusion in biological tissues are inversely correlated to the tissue cellularity and the integrity of the cell membranes (37,38). Several authors have already reported decreased ADC among various malignant lesions due to dense cellularity and large cellular size (16–23,37,38). Matsuki et al (24) also reported that ADCs of urinary bladder cancers were lower than those of the surrounding structures. In our study, the mean ADC of G3 tumors was significantly lower than that of G1 and G2 tumors, and all G3 tumors had an ADC less than 1.0×10^{-3} mm^2/sec. Because both ADC and histologic grade are independently influenced by several factors other than the cellular density, the correlation between the two could be limited, but the ADC may still in part predict the histologic grade of bladder cancer.

Our study had a number of limitations. Tumors were divided into only four grades, whereas previous investigators classified them into five or more groups. This difference in classification might have led to higher accuracy in our study compared to that in previous reports (3–9). In addition, the distribution of T stages was uneven, with a large number of T1 or lower tumors and a small number of pT2 tumors; therefore, larger studies are warranted to more fully define the role of DW imaging in T staging of bladder tumors. However, our primary objectives were to discriminate T1 or lower tumors from T2 or higher tumors and to assess the sensitivity, specificity, and accuracy of MR imaging, so the sample sizes were considered acceptable. There is a possibility that inflammatory changes due to prior treatment or biopsy before MR imaging affected evaluation in some cases (39). Finally, the radiologic-pathologic correlation was not perfect because some of the specimens obtained by TUR were not available, and the cut surfaces on surgical specimens were not always completely identical to those seen on MR images.

In conclusion, DW images appear to provide useful information for evaluating T stage in patients with bladder cancer, particularly for differentiating T1 or lower tumors from T2 or higher tumors, and a low ADC appears to suggest that the tumor is more likely to be G3. Because DW imaging does not re-

quire a contrast agent and images become available quickly, it could be a useful adjunct to preoperative evaluation with MR imaging.

References

1. Josephson D, Pasin E, Stein JP. Superficial bladder cancer. II. Management. Expert Rev Anticancer Ther 2007;7:567–581.
2. Sherif A, Jonsson MN, Wiklund NP. Treatment of muscle-invasive bladder cancer. Expert Rev Anticancer Ther 2007;7:1279–1283.
3. Tekes A, Kamel I, Imam K, et al. Dynamic MRI of bladder cancer: evaluation of staging accuracy. AJR Am J Roentgenol 2005;184:121–127.
4. Hayashi N, Tochigi H, Shiraishi T, Takeda K, Kawamura J. A new staging criterion for bladder carcinoma using gadolinium-enhanced magnetic resonance imaging with an endorectal surface coil: a comparison with ultrasonography. BJU Int 2000;85:32–36.
5. Scattoni V, Da Pozzo LF, Colombo R, et al. Dynamic gadolinium-enhanced magnetic resonance imaging in staging of superficial bladder cancer. J Urol 1996;155:1594–1599.
6. Barentsz JO, Jager G, Mugler JP III, et al. Staging urinary bladder cancer: value of T1-weighted three-dimensional magnetization prepared–rapid gradient-echo and two-dimensional spin-echo sequences. AJR Am J Roentgenol 1995;164:109–115.
7. Kim B, Semelka RC, Ascher SM, Chalpin DB, Carroll PR, Hricak H. Bladder tumor staging: comparison of contrast-enhanced CT, T1- and T2-weighted MR imaging, dynamic gadolinium-enhanced imaging, and late gadolinium-enhanced imaging. Radiology 1994;193:239–245.
8. Narumi Y, Kadota T, Inoue E, et al. Bladder tumors: staging with gadolinium-enhanced oblique MR imaging. Radiology 1993;187:145–150.
9. Tanimoto A, Yuasa Y, Imai Y, et al. Bladder tumor staging: comparison of conventional and gadolinium-enhanced dynamic MR imaging and CT. Radiology 1992;185:741–747.
10. Prince MR, Zhang H, Morris M, et al. Incidence of nephrogenic systemic fibrosis at two large medical centers. Radiology 2008; 248:807–816.
11. Tsushima Y, Takano A, Taketomi-Takahashi A, Endo K. Body diffusion-weighted MR imaging using high *b*-value for malignant tumor screening: usefulness and necessity of referring to T2-weighted images and creating fusion images. Acad Radiol 2007;14:643–650.
12. Ichikawa T, Erturk SM, Motosugi U, et al. High-*b*-value diffusion-weighted MRI in colorectal cancer. AJR Am J Roentgenol 2006; 187:181–184.
13. Ichikawa T, Erturk SM, Motosugi U, et al. High-*b* value diffusion-weighted MRI for detecting pancreatic adenocarcinoma: preliminary results. AJR Am J Roentgenol 2007; 188:409–414.
14. Haider MA, van der Kwast TH, Tanguay J, et al. Combined T2-weighted and diffusion-weighted MRI for localization of prostate cancer. AJR Am J Roentgenol 2007;189: 323–328.
15. Kuroki-Suzuki S, Kuroki Y, Nasu K, Nawano S, Moriyama N, Okazaki M. Detecting breast cancer with non-contrast MR imaging: combining diffusion-weighted and STIR imaging. Magn Reson Med Sci 2007;6:21–27.
16. Muller MF, Prasad P, Siewert B, Nissenbaum MA, Raptopoulos V, Edelman RR. Abdominal diffusion mapping with use of a whole-body echo-planar system. Radiology 1994; 190:475–478.
17. Yoshino N, Yamada I, Ohbayashi N, et al. Salivary glands and lesions: evaluation of apparent diffusion coefficients with split-echo diffusion-weighted MR imaging—initial results. Radiology 2001;221:837–842.
18. Namimoto T, Yamashita Y, Sumi S, Tang Y, Takahashi M. Focal liver masses: characterization with diffusion-weighted echo-planar MR imaging. Radiology 1997;204:739–744.
19. Yamada I, Aung W, Himeno Y, Nakagawa T, Shibuya H. Diffusion coefficients in abdominal organs and hepatic lesions: evaluation with intravoxel incoherent motion echo-planar MR imaging. Radiology 1999;210:617–623.
20. Taouli B, Vilgrain V, Dumont E, Daire JL, Fan B, Menu Y. Evaluation of liver diffusion isotropy and characterization of focal hepatic lesions with two single-shot echo-planar MR imaging sequences: prospective study in 66 patients. Radiology 2003;226:71–78.
21. Squillaci E, Manenti G, Cova M, et al. Correlation of diffusion-weighted MR imaging with cellularity of renal tumours. Anticancer Res 2004;24:4175–4179.
22. Matoba M, Tonami H, Kondou T, et al. Lung carcinoma: diffusion-weighted MR imaging-preliminary evaluation with apparent diffusion coefficient. Radiology 2007;243:570–577.
23. Woodhams R, Matsunaga K, Kan S, et al. ADC mapping of benign and malignant breast tumors. Magn Reson Med Sci 2005;4:35–42.
24. Matsuki M, Inada Y, Tatsugami F, et al. Diffusion-weighted MR imaging for urinary bladder carcinoma: initial results. Eur Radiol 2007;17:201–204.
25. Tweedle MF. Physicochemical properties of gadoteridol and other magnetic resonance contrast agents. Invest Radiol 1992;27(suppl 1):S2–S6.
26. Sobin LH, Wittekind CH, eds. International Union Against Cancer (UICC): TNM classification of malignant tumors. New York, NY: Wiley-Liss, 1997; 170–173.
27. Fisher MR, Hricak H, Tanagho EA. Urinary bladder MR imaging. II. Neoplasm. Radiology 1985;157:471–477.
28. Buy JN, Moss AA, Guinet C, et al. MR staging of bladder carcinoma: correlation with pathologic findings. Radiology 1988;169:695–700.
29. Rholl KS, Lee JK, Heiken JP, Ling D, Glazer HS. Primary bladder carcinoma: evaluation with MR imaging. Radiology 1987;163:117–121.
30. Narumi Y, Kadota T, Inoue E, et al. Bladder wall morphology: in vitro MR imaging-histopathologic correlation. Radiology 1993; 187:151–155.
31. Bammer R. Basic principles of diffusion-weighted imaging. Eur J Radiol 2003;45:169–184.
32. Mostfi FK, Sobin LH, Torloni H. Histological typing of urinary bladder tumours. Geneva, Switzerland: World Health Organization, 1973.
33. Landis JR, Koch CG. The measurement of observer agreement for categorical data. Biometrics 1977;33:159–174.
34. Rosner B. Two-sample test for binomial proportions for matched-pair data (McNemar's test). In: Rosner B, ed. Fundamentals of biostatistics. 5th ed. Pacific Grove, Calif: Duxbury, 2000; 376–384.
35. Dorfman DD, Berbaum KS, Metz CE. Receiver operating characteristic rating analysis: generalization to the population of readers and patients with the jackknife method. Invest Radiol 1992;27:723–731.
36. Saito W, Amanuma M, Tanaka J, Heshiki A. Histopathological analysis of a bladder cancer stalk observed on MRI. Magn Reson Imaging 2000;18:411–415.
37. Koh DM, Collins DJ. Diffusion-weighted MRI in the body: applications and challenges in oncology. AJR Am J Roentgenol 2007;188: 1622–1635.
38. Sugahara T, Korogi Y, Kochi M, et al. Usefulness of diffusion-weighted MRI with echo-planar technique in the evaluation of cellularity in gliomas. J Magn Reson Imaging 1999;9:53–60.
39. Barentsz JO, Jager GJ, van Vierzen PB, et al. Staging urinary bladder cancer after transurethral biopsy: value of fast dynamic contrast-enhanced MR imaging. Radiology 1996; 201:185–193.